

Multidentate Phenanthroline Ligands Containing Additional Donor Moieties and Their Resulting Cu(I) and Ru(II) Photosensitizers: A Comparative Study

Martin Rentschler,[†] Marie-Ann Schmid,[†] Wolfgang Frey, Stefanie Tschierlei,^{*} and Michael Karnahl^{*}



Cite This: <https://dx.doi.org/10.1021/acs.inorgchem.9b03687>



Read Online

ACCESS |



Metrics & More

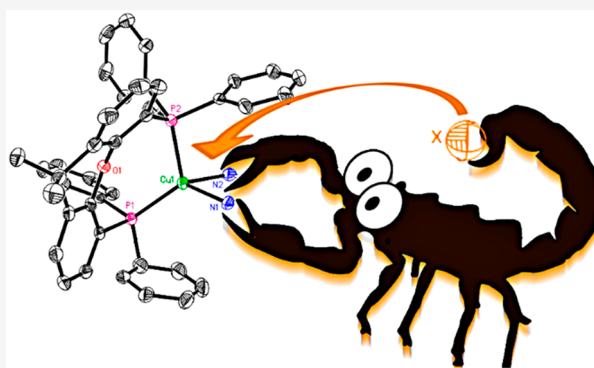


Article Recommendations



Supporting Information

ABSTRACT: To bind or not to bind: Driven by the motivation to increase the (photo)stability of traditional Cu(I) photosensitizers, multidentate diimine ligands, which contain two additional donor sites, were designed. To this end, a systematic series of four 1,10-phenanthroline ligands with either OR or SR (R = ⁱPr or Ph) donor groups at the 2 and 9 positions and their resulting hetero- and homoleptic Cu(I) complexes were prepared. In addition, the related Ru(II) complexes were also synthesized to study the effect of another metal center. In the following, a combination of NMR spectroscopy and X-ray analysis was used to evaluate the impact of the additional donor moieties on the coordination behavior. Most remarkably, for the homoleptic bis(diimine)copper(I) complexes, a pentacoordinated copper center, corresponding to a (4 + 1)-fold coordination mode, was found in the solid state. This additional binding is the first indication that the extra donor might also occupy a free coordination site in the excited-state complex, modifying the nature of the excited states and their respective deactivation processes. Therefore, the electrochemical and photophysical properties of all novel complexes (in total 13) were studied in detail to assess the potential of these photosensitizers for future applications within solar energy conversion schemes. Finally, the photostabilities and a potential degradation mechanism were analyzed for representative samples.



INTRODUCTION

Photosensitizers based on transition-metal complexes have received intense attention owing to their advantageous photophysical and electrochemical properties.^{1–5} Consequently, these compounds are already successfully used for a variety of photonic applications such as dye-sensitized solar cells (DSSCs)^{6,7} or organic light-emitting diodes (OLEDs)^{8,9} and for photoredox catalysis.^{10–15} In this respect, particularly ruthenium(II) polypyridine complexes have been studied in detail for decades because of their high chemical stability, strong absorption of visible light, and tunable redox behavior.^{1,5,16–18} However, ruthenium is a rare and expensive noble metal (only 0.001 ppm in the Earth's crust), which complicates the broad application of Ru(II) photosensitizers in solar-energy conversion schemes.

For this reason, luminescent Cu(I) complexes have become more and more interesting as a promising alternative.^{19–24} Nevertheless, a basic distinction must be made between homo- and heteroleptic Cu(I) compounds, which bear different pros and cons.^{2,22,23,25} Homoleptic bis(diimine)copper(I) complexes of the type [Cu(N[^]N)₂]⁺, where N[^]N indicates a chelating diimine ligand, are commonly characterized by a decent absorption in the visible range and a high

stability.^{2,26–28} Unfortunately, the lifetime of the triplet excited state is usually only on the order of a few nanoseconds, and the quantum yields are often much lower than those of the competing Ru(II) photosensitizers.^{2,22,29}

In comparison to their homoleptic counterparts, heteroleptic diiminediphosphinecopper(I) complexes with the general formula [(P[^]P)Cu(N[^]N)]⁺ possess increased emission quantum yields and excited-state lifetimes.^{23,24,30,31} These compounds can also be tuned in a wider range because of the presence of two different types of ligands. However, as a major drawback, these heteroleptic Cu(I) complexes suffer from a reduced photostability.^{28,32–34} Several studies evidenced that in solution, under reaction conditions, a dissociation of the diphosphine ligand occurs.^{28,32–35}

As a common feature, all Cu(I) complexes possess a (distorted) tetrahedral ground-state structure.^{2,23} Upon light

Special Issue: Light-Controlled Reactivity of Metal Complexes

Received: December 19, 2019

excitation, a metal-to-ligand charge-transfer (MLCT) transition from the 3d orbital of Cu(I) to the π^* orbital of the diimine ligand takes place.^{23,29,36,37} This causes a formal oxidation from Cu(I) to Cu(II) and a single-electron reduction of one diimine ligand. As a result, a significant change in the coordination geometry and a flattening toward a more square-planar structure occurs, corresponding to the 3d⁹ configuration of Cu(II).^{23,29,36–38} In this flattened geometry, the complex is more open for a nucleophilic attack by solvent molecules or counterions, leading to a pentacoordinated excited-state complex (exciplex).^{2,29,37} This exciplex is then efficiently deactivated via nonemissive deactivation pathways, causing short excited-state lifetimes and restricting the applicability.

It is known that sterically demanding and rigid ligands can suppress flattening distortion upon photoexcitation and shield the copper center against nucleophilic attack.^{20,23,24,30} As a possible alternative, multidentate ligands could be used that occupy the free coordination site in the exciplex with an additional donor from the beginning (see Figure 1).^{35,39,40}

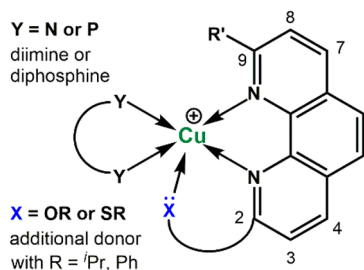
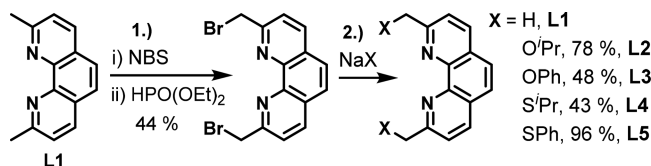


Figure 1. General concept of this study investigating the impact of an additional donor moiety on the coordination behavior of the corresponding homo- and heteroleptic Cu(I) complexes.

Thereby, a nucleophilic attack might be prevented in the excited state. The understanding of this issue and of the coordination behavior of multidentate diimine ligands is the main goal of the present study.

For this purpose, four phenanthroline ligands, which contain two additional donor moieties in the 2 and 9 positions, were designed (see Scheme 1). As suitable donor functions, OR and

Scheme 1. Depiction of the Two-Step Synthesis Procedure of the Ligands L2–L5^a



^aReaction conditions: (1) (i) NBS, MeCN, reflux, 18 h; (ii) HPO(OEt)₂, ⁱPrNEt₃, THF, 0 °C to rt; (2) NaX, solvent, reflux, 4–24 h.

SR groups (with R = ⁱPr or Ph) were chosen because of their good availability and the fact that substituents in this position are known to improve the photophysical properties of the resulting Cu(I) complexes.^{20,23,24,30} Furthermore, these chalcogen elements only carry one additional substituent R compared to phosphines PR₂. As a consequence, the OR and SR donor groups are less sterically demanding, which may facilitate a 5-fold coordination (see Figure 1). Moreover, the sulfur moiety is less prone to undergoing an unwanted

oxidation reaction compared to the corresponding phosphines.^{41,42}

After the successful synthesis of the multidentate phenanthroline ligands L2–L5, the corresponding hetero- and homoleptic Cu(I) complexes Cu2–Cu5 and Cu2'–Cu5' (see Figure 2) were prepared. For comparison, also the related

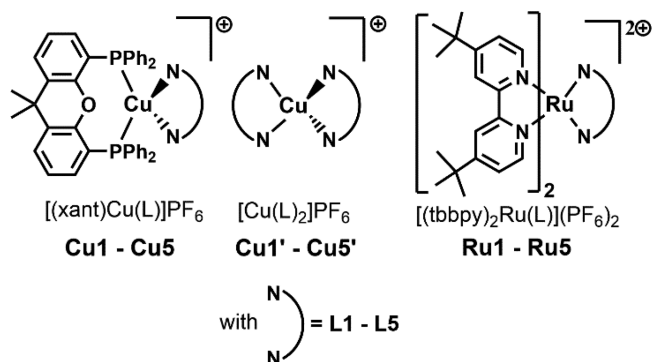


Figure 2. Overview and numbering of the different Cu(I) and Ru(II) complexes that were studied.

Ru(II) photosensitizers Ru2–Ru5 with the general formula [(tbbpy)₂Ru(L)]²⁺ (with tbbpy = 4,4'-di-*tert*-butyl-2,2'-bipyridine) were made. The three reference complexes Cu1, Cu1', and Ru1 with the 2,9-dimethyl-1,10-phenanthroline ligand L1 were used to systematically evaluate the electronic and steric effects of the additional donor moiety. It should be noted that, although there are already a large variety of ruthenium(II) phenanthroline complexes, the reference Ru1 was not yet presented. All in all, crystals suitable for X-ray analysis were obtained for 8 of the 13 new complexes (in total 15 complexes), which allowed for a comprehensive elucidation of the coordination behavior.

In addition, the photophysical (i.e. absorption and emission behavior, excited-state lifetimes, and emission quantum yields) and electrochemical properties were studied in detail for all complexes. As a result, structure–property relationships have been identified, providing valuable information for future studies. Interestingly, the OⁱPr group has been proven as the best substituent in terms of the resulting photophysical and electrochemical properties. This can be understood by a proposed decomposition mechanism of the other ligands under reductive conditions.

RESULTS AND DISCUSSION

Synthesis and Structural Characterization. *Synthesis of the Phenanthroline-Derived Ligands.* Starting from the commercially available 2,9-dimethyl-1,10-phenanthroline ligand L1, 2,9-dibromomethyl-1,10-phenanthroline was prepared in two steps following a known literature procedure.⁴³ The obtained dibrominated phenanthroline derivative serves then as a universal intermediate that can be further functionalized by nucleophilic substitution of the two bromine atoms. Applying the sodium salts of either (thio)isopropyl alcohol or (thio)phenol as nucleophiles results in the phenanthroline ligands L2–L5 containing two (thio)ether functionalities each (see Scheme 1) with 48–96% yield. Only L4 (SⁱPr, 43%) had to be additionally recrystallized from *n*-hexane to increase purity. The ligand L3 (OPh) was already presented in the literature but prepared by a different procedure.⁴⁴

Table 1. Selected Crystallographic Bond Lengths (pm) and Angles (deg) of the Hetero- and Homoleptic Cu(I) Complexes **Cu1**, **Cu2**, **Cu4**, and **Cu1'–Cu5'**^a

	Cu1(space group P1) ^{b,c}	Cu2(space group P1)	Cu4(space group P1)		Cu1'(space group P2 ₁ /c) ^{b,d}	Cu2'(space group C2/c)	Cu3'(space group P1)	Cu4'(space group P1)	Cu5'(space group P1)
Cu–N1	208.4(3)	208.4(4)	210.7(3)	Cu–N1	202.8(2)	202.06(14)	203.6(3)	205.3(3)	204(1)
Cu–N2	211.2(3)	210.6(4)	210.2(3)	Cu–N2	204.2(2)	202.06(14)	204.2(2)	202.0(3)	204(1)
Cu–P1	226.26(11)	224.94(13)	225.34(11)	Cu–N3	205.3(2)	204.80(14)	204.1(3)	206.9(3)	200.0(9)
Cu–P2	228.63(13)	231.27(13)	230.48(11)	Cu–N4	207.0(2)	204.81(14)	203.5(2)	201.0(3)	205(1)
Cu–X1		470.3(4)	506.1(1)	Cu–X1		352.31(13)	328.9(2)	389.7(1)	376.3(4)
Cu–X2		447.4(4)	483.2(1)	Cu–X2		462.43(13)	350.3(2)	420.2(2)	392.3(4)
				Cu–X3		352.31(13)	457.3(2)	496.8(2)	404.0(5)
				Cu–X4		462.43(13)	472.7(2)	486.3(2)	394.6(5)
N1–Cu–N2	80.53(13)	80.97(15)	79.92(13)	N1–Cu–N2	81.78(8)	82.53(6)	82.4(1)	81.8(1)	82.4(5)
P1–Cu–P2	112.93(4)	120.43(5)	116.59(4)	N3–Cu–N4	81.95(8)	82.53(6)	82.2(1)	82.4(1)	83.0(4)
N1–Cu–P1	108.77(9)	119.73(11)	121.55(10)	N1–Cu–N3	110.75(8)	134.40(8)	133.8(1)	117.5(1)	128.4(5)
N1–Cu–P2	120.33(9)	102.33(11)	103.1(1)	N1–Cu–N4	126.67(8)	121.75(5)	123.4(1)	121.6(1)	124.4(5)
N2–Cu–P1	120.33(9)	126.99(11)	127.1(1)	N2–Cu–N3	128.42(8)	121.75(5)	117.1(1)	121.2(1)	124.9(5)
N2–Cu–P2	118.59(9)	97.86(10)	101.3(1)	N2–Cu–N4	132.11(8)	118.50(8)	123.6(1)	136.5(1)	119.0(5)
P–P–N–N	76.9	85.9	87.8	N–N–N–N	79.4	86.9	82.3	86.3	88.7

^aThe values in parentheses represents the experimental estimated standard deviation of the measurement. ^b**Cu1** and **Cu1'** were already published earlier but are given here for comparison. ^cReference 45. ^dReference 49.

Synthesis of the Cu(I) and Ru(II) Complexes. After the successful synthesis of multidentate phenanthroline ligands **L2–L5**, which contain two additional chalcogen donor moieties, we were interested in their coordination behavior. Therefore, these ligands were coordinated to different potentially photoactive metal centers (see [Figure 2](#)). The heteroleptic Cu(I) complexes **Cu1–Cu5** of the type [(xant)-Cu(L)]PF₆ (with xant = xantphos) as well as their homoleptic counterparts **Cu1'–Cu5'** [Cu(L)₂]PF₆ and the heteroleptic Ru(II) complexes **Ru1–Ru5** with the general formula [(tbbpy)₂Ru(L)](PF₆)₂ (with tbbpy = 4,4'-di-*tert*-butyl-2,2'-bipyridine) were prepared to evaluate the potential of these phenanthroline-derived ligands.

The heteroleptic Cu(I) complexes **Cu1–Cu5** (see [Figure 2](#)) were synthesized following a procedure that was established for these types of complexes previously.^{21,30,45} First, the xantphos ligand was coordinated to the copper center by refluxing a mixture of [Cu(MeCN)₄]PF₆ and xantphos in dichloromethane for 16 h under inert conditions. Then, the respective phenanthroline ligands **L1–L5**, dissolved in dichloromethane, was added dropwise at 0 °C. The solution was again refluxed for 4 h, whereby a significant yellow coloring occurred. After cooling to room temperature, the desired complexes were precipitated by the addition of *n*-hexane. Complexes **Cu1–Cu5** were received in 37–86% yield.

The homoleptic Cu(I) complexes **Cu1'–Cu5'** (see [Figure 2](#)) were prepared by following a previously reported procedure.^{45,46} For this purpose, the copper precursor [Cu(MeCN)₄]PF₆ and the respective phenanthroline ligands **L1–L5** were dissolved in dichloromethane and heated to reflux for 3 h. After cooling to room temperature, the desired complexes were precipitated by the addition of *n*-hexane. Complexes **Cu1'–Cu5'** were isolated in 43–87% yield. It should be noted that, for complex **Cu3'**, a crystal structure already existed, but no further synthetic details and structural, photophysical, or electrochemical data were provided.⁴⁴

For the synthesis of the heteroleptic Ru(II) complexes **Ru1–Ru5** (see [Figure 2](#)), two different strategies were

applied.^{47,48} However, all Ru(II) complexes were prepared by refluxing a mixture of [(tbbpy)₂RuCl₂] and the respective phenanthroline derivatives **L1–L5** in ethanol and water. Further synthetic details are given in the [Supporting Information \(SI\)](#). Complexes **Ru1–Ru5** were obtained as orange-to-red solids in 38–86% yield.

After their synthesis, all ligands and complexes were fully characterized by ¹H, ¹³C, and ³¹P NMR spectroscopy, high-resolution mass spectrometry (HRMS), and elemental analysis (see the [SI](#)). The expected elemental composition and purity were confirmed by the obtained HRMS and elemental analysis. Furthermore, the NMR spectra are in accordance with the proposed structures (see the [SI](#), Chapter 4). Interestingly, the heteroleptic Cu(I) complexes **Cu2–Cu5** with the additional donor moieties at the phenanthroline ligand showed no significant deviation in the ³¹P NMR signal ($\delta = -13.2$ to -13.9 ppm, measured in acetonitrile-*d*₃) compared to complex **Cu1** ($\delta = -13.4$ ppm)⁴⁴ without additional donors. This indicates that there is no variation in the coordination behavior of the copper center because a change in the type or geometry of coordination would most likely also cause a shift in the ³¹P NMR signal. This nonaltered coordination behavior has been further confirmed by crystal structure analysis and is discussed below.

In the ¹H NMR spectra of the homoleptic Cu(I) complexes **Cu2'–Cu5'**, only one set of signals is present. Therefore, the interaction between one of the additional donor atoms and the copper center that is observed in the crystal structure of these complexes is weak and undergoes a fast exchange at higher rates than the NMR time scale. Even temperature-dependent ¹H NMR measurements of **Cu2'** in a methanol-*d*₄ solution, performed in the range from 303 to 183 K, resulted in no obvious shift of the ¹H NMR signals and no occurrence of additional signals because they would be expected for nonequivalent protons. Only a broadening of the ligand signals and a shift of the solvent signal are observed at lower temperatures (see [Figure S4.18](#)).

In the ^1H NMR spectra of the Ru(II) complexes **Ru2**–**Ru5**, a splitting of the signals belonging to the benzylic protons is present. Furthermore, for complexes **Ru2** and **Ru4**, also a splitting of the signals belonging to the isopropyl methyl groups in the respective ^1H NMR spectra is observed (see Figures S4.14 and S4.16). This suggests a stereogenic center at the neighboring donor atoms, which could be formed by the coordination of both additional donor atoms to the Ru(II) center. The subsequent crystal structure analysis of **Ru3** (OPh) showed that the diastereotopic environment is created by the coordination behavior of the ligand **L3**. **L3** coordinates in a defined way, where the additional donor atoms point away from the ruthenium center.

Single crystals suitable for X-ray analysis could be obtained for 8 of the 13 novel complexes (see Tables 1 and 2) by

Table 2. Selected Crystallographic Bond Lengths (pm) and Angles (deg) of the Ru(II) Complexes **Ru1 and **Ru3**^a**

	Ru1 (space group $P2_1/c$)	Ru3_a (space group $P1$) ^b	Ru3_b (space group $P1$) ^b
Ru–N1	210.4(5)	206(1)	213(1)
Ru–N2	210.0(4)	214.6(9)	214(1)
Ru–N3	206.8(5)	204(1)	203(1)
Ru–N4	206.3(5)	206(1)	207(1)
Ru–N5	203.8(4)	207(1)	204(1)
Ru–N6	205.9(5)	212.0(9)	208.0(9)
Ru–X1		485(1)	483(1)
Ru–X2		486(1)	490(1)
N1–Ru–N2	79.4(2)	80.1(4)	78.9(5)
N3–Ru–N4	171.3(2)	79.0(5)	78.2(4)
N5–Ru–N6	79.3(2)	78.6(5)	78.0(5)
N1–Ru–N3	92.9(2)	95.2(4)	97.4(5)
N1–Ru–N4	93.2(2)	173.4(5)	175.4(5)
N1–Ru–N5	101.4(2)	87.3(5)	88.6(5)
N1–Ru–N6	171.5(2)	102.1(5)	102.5(5)
N2–Ru–N3	88.3(2)	88.9(4)	92.4(5)
N2–Ru–N4	98.8(2)	102.5(5)	102.4(5)
N2–Ru–N5	177.3(2)	94.5(5)	93.1(5)
N2–Ru–N6	100.3(2)	172.6(5)	170.9(5)

^aThe values in parentheses represent the experimental estimated standard deviation of the measurement. ^b**Ru3** crystallized in a lattice with two twinned units of the respective complex. The two units are referred as **Ru3_a** and **Ru3_b**.

layering a dichloromethane solution of the respective complex with ethanol and *n*-hexane. As a result, structural data were received for the heteroleptic Cu(I) complexes **Cu2** and **Cu4**, the homoleptic Cu(I) complexes **Cu2'**–**Cu5'**, and the Ru(II) complexes **Ru1** and **Ru3** and are discussed below. Interestingly, almost all Cu(I) compounds crystallize in a triclinic crystal system with the space group $P\bar{1}$ (see Table 1).

Crystal Structure Analysis of the Heteroleptic Copper Complexes. Both Cu(I) complexes **Cu2** and **Cu4** (see Figure 3) possess a distorted tetrahedral ground-state structure, which is commonly observed for this class of compounds.^{24,30,45} This is mainly caused by the bulky and rigid xantphos ligand and the large difference in the bite angles of the diimine and diphosphine [e.g., for **Cu2**, N1–Cu–N2 = 80.97(15)° and P1–Cu–P2 = 120.43(5)°]. With 76.9° (**Cu1**), 85.9° (**Cu2**), and 87.8° (**Cu4**), the angle between the two ligand planes, which are spanned through the chelating heteroatoms and

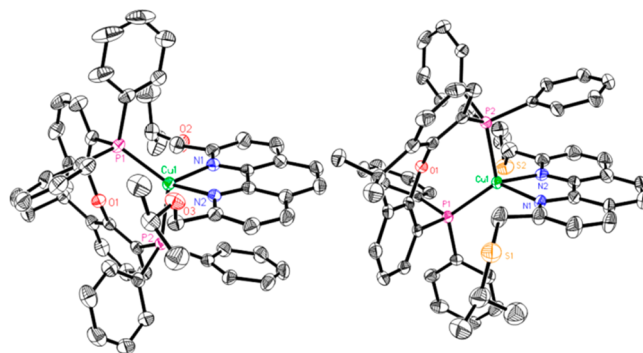


Figure 3. Solid-state structures (ORTEP representation) of the heteroleptic Cu(I) complexes **Cu2** (left) and **Cu4** (right). Ellipsoids are drawn at 50% probability. Hydrogen atoms, PF_6^- counteranions, and solvent molecules are omitted for clarity.

copper center, differs clearly from the 90° of an ideal tetrahedron (see Table 1). However, because of the additional bulkiness of the OR and SR substituents at the 2 and 9 positions, **Cu2** and **Cu4** appear less distorted than the reference complex **Cu1** with methyl groups only. A comparison of further structural parameters of **Cu2**, **Cu4**, and **Cu1** (see Table 1) does not show major differences with respect to the basic coordination geometry (e.g., N1–Cu–N2 = 80.53(13)° for **Cu1** and 80.97(15)° for **Cu2**; Cu–N1 = 208.4(3) pm for **Cu1** and 208.4(4) pm for **Cu2**). This indicates a small impact of the substituents at 1,10-phenanthroline on the general structure around the Cu(I) center. Most importantly, in the solid-state structures of the heteroleptic Cu(I) complexes **Cu2** (OⁱPr) and **Cu4** (SⁱPr), the additional donor functions point away from the copper center (see Figure 3), resulting in Cu–X distances of ≥ 4.5 Å. This clearly shows that there is no interaction between the Cu(I) center and additional donor atoms in the heteroleptic complexes. Consequently, no change in the ^{31}P NMR chemical shift was observed when the additional donor functions were introduced.

Crystal Structure Analysis of the Homoleptic Copper Complexes **Cu2'–**Cu5'**.** All homoleptic Cu(I) complexes **Cu2'**–**Cu5'** could be examined by X-ray crystallography (see Figure 4), and they show again the typical distorted tetrahedral structure.^{2,22,49} In addition, the reference complex **Cu1'** exhibits the smallest angle between the two ligand planes (79.4°) compared to the substituted derivatives **Cu2'**–**Cu5'** (82.3–88.7°; see Table 1). Hence, **Cu1'** features the largest distortion from the tetrahedral coordination sphere, whereas the additional substituents in **Cu2'**–**Cu5'** reduce the extent of the flattening. The different types of substituents (OⁱPr, OPh, SⁱPr, and SPh) have almost no influence on the Cu–N distances (e.g., Cu–N1 = 203.6(3) pm for **Cu3'**, 205.3(3) pm for **Cu4'**, and 204(1) pm for **Cu5'**) and the bite or tetrahedral angles, which are in the same range for all complexes (see Table 1). Special attention was then paid to the Cu–X distances (X=OⁱPr, OPh, SⁱPr, or SPh). As a main difference to the heteroleptic Cu(I) complexes, all homoleptic compounds **Cu2'**–**Cu5'** possess one Cu–X distance, which is significantly shortened. For instance, in **Cu3'**, the Cu–O1 distance is 328.9(2) pm, whereas Cu–O3 is 457.3(2) pm. This indicates a weak interaction between the copper center and one of the additional donor atoms. It should be noted that the crystal structure of complex **Cu2'** has a higher symmetry than

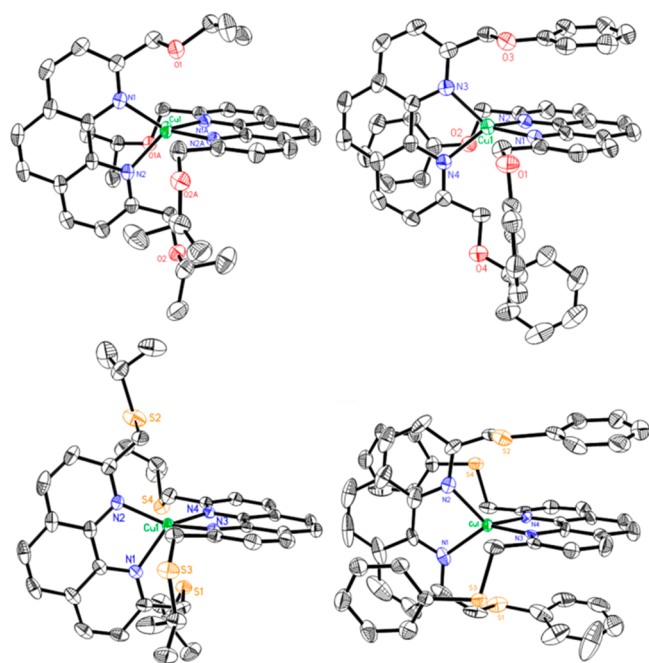


Figure 4. Solid-state structures (ORTEP representation) of the homoleptic Cu(I) complexes **Cu2'** (top left), **Cu3'** (top right), **Cu4'** (bottom left), and **Cu5'** (bottom right). Ellipsoids are drawn at 50% probability. Hydrogen atoms, PF_6^- counteranions, and solvent molecules are omitted for clarity.

the other homoleptic Cu(I) complexes, which leads to two shortened Cu–X distances instead of only one. For complexes **Cu2'**, **Cu4'**, and **Cu5'**, it was further observed that the shortened Cu–X distance is accompanied by an elongation of the respective H_2C –X bond (see Table S3) because this is the longest H_2C –X distance within the complex [e.g., for **Cu2'**, 142.3(3) pm compared to a distance of 141.5(2) pm, and for **Cu4'**, 182.4(6) pm compared to distances of 180.1(6)–182.0(6) pm].

Crystal Structure Analysis of the Heteroleptic Ruthenium Complexes. Crystals suitable for X-ray analysis were obtained for the Ru(II) complexes **Ru1** and **Ru3**. It should be noted that complex **Ru3** crystallized in a lattice with two twinned units, which are referred to as **Ru3_a** and **Ru3_b** (see Table 2). Structural analysis of **Ru1** and **Ru3** (see Figure 5) revealed a conventional octahedral coordination environment around the ruthenium center, which is common for these Ru(II)

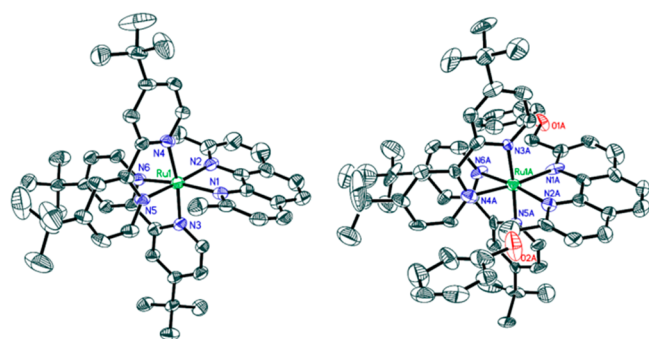


Figure 5. Solid-state structures (ORTEP representation) of the Ru(II) complexes **Ru1** and **Ru3**. Ellipsoids are drawn at 50% probability. Hydrogen atoms, PF_6^- counteranions, and solvent molecules are omitted for clarity.

compounds.^{50–52} Deviations from an ideal octahedron are caused by the bite angles of the three diimine ligands that are all smaller than 90° . The Ru–N bond lengths are between 203(1) and 214.6(9) pm. The N–Ru–N bite angles at the phenanthroline ligand are between $78.9(5)^\circ$ and $80.1(4)^\circ$. The N–Ru–N angles, with one of the nitrogen atoms being part of the phenanthroline ligand, are between $87.3(5)^\circ$ and $102.5(5)^\circ$ for neighboring nitrogen atoms and between $170.9(5)$ and $177.3(2)$ for opposing nitrogen atoms.

Crystal structure analysis shows that there is no coordination of the additional donor atoms to the ruthenium center, although it has been indicated by the ^1H NMR spectra. The additional donor atoms do all point away from the ruthenium center (see Figure 5). As evidenced by the NMR data, the benzylic protons do have distinct diastereotopic environments, but they are not caused by the coordination of an additional donor to the ruthenium center. To minimize steric repulsion, the additional donor atoms point away from the metal center and are in plane with the phenanthroline backbone. This leads to one of the benzylic hydrogen atoms being above the phenanthroline plane, while the other one is below. The helical arrangement of the tbbpy ligands of the $\text{Ru}(\text{tbbpy})_2$ fragment causes the two benzylic protons to have nonequivalent chemical surroundings (see Figure S4.15).

Photophysical Studies. All complexes exhibit pronounced absorption bands in the UV region at 280 nm [for the Cu(I) complexes] and 300 nm [for the Ru(II) complexes], which can be assigned to ligand-centered (LC) transitions.^{1,23} The absorption bands attributed to the MLCT transitions are generally broader and appear between 350 and 400 nm for **Cu1**–**Cu5** or between 400 and 500 nm for **Cu1'**–**Cu5'** and **Ru1**–**Ru5** (see Figure 6).^{23,29}

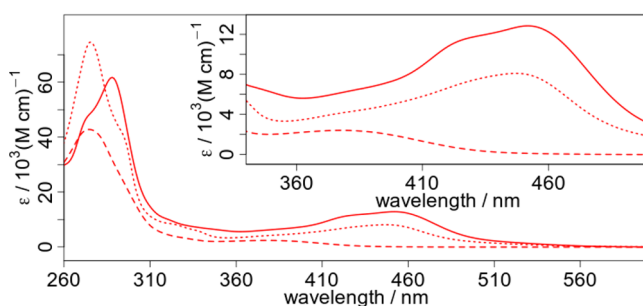


Figure 6. UV/vis absorption spectra (attenuation coefficient) of **Cu2** (dashed), **Cu2'** (dotted), and **Ru2** (solid) in acetonitrile. **Cu2**, **Cu2'**, and **Ru2** were selected as characteristic representatives of their substance class (for the other UV/vis spectra, see the SI, Chapter 6). The inset enlarges the MLCT region.

The maxima of the MLCT absorption of the heteroleptic Cu(I) complexes **Cu2**–**Cu5** are localized around 380 nm with a slight bathochromic shift for the thioether-functionalized complexes **Cu4** (S^iPr , 384 nm) and **Cu5** (S^iPh , 382 nm; see Table 3). The intensities of these MLCT bands are lower compared to that of the reference **Cu1**; e.g., the attenuation coefficient of **Cu4** is halved. Related heteroleptic Cu(I) complexes containing 6-alkylthio- or 6-phenylthio-substituted 2,2'-bipyridine ligands show similar behavior.⁵³ The same trend is observed for the homoleptic counterparts **Cu2'**–**Cu5'**. Again the attenuation coefficients are somewhat decreased compared to the reference complex **Cu1'** with methyl substituents only. The absorption bands of the thioether-

Table 3. Summary of the Photophysical and Electrochemical Properties of the Different Complexes (in Acetonitrile) and Ligands (in Dichloromethane for Solubility Reasons)

compound	$\lambda_{\text{max,abs}}$, nm (ϵ , $\times 10^3$ M $^{-1}$ cm $^{-1}$)	$\lambda_{\text{max,em}}$, nm (τ , ns)	Φ , %	$E_{1/2,\text{red}}$, V	$E_{1/2,\text{ox}}$, V
Cu1	379 (3.12)	551 (64 ^a)		−2.10	0.40
Cu2	378 (2.39)	540 (15)	0.23	−2.06	0.33, ^c 0.95
Cu3	380 (1.94)	539 (10)		−1.98 ^c	1.09 ^c
Cu4	384 (1.43)	535 (14)		−2.46, ^c −2.06 ^c	0.96, ^c 1.22 ^c
Cu5	382 (1.94)	535 (13)		−1.84 ^c	0.13, ^c 0.27, ^c 0.92 ^c
Cu1'	455 (7.95) ^b			−2.11 ^{c,d}	0.29 ^d
Cu2'	447 (8.1)			−2.26, −2.04	0.12
Cu3'	449 (6.77)			−2.38, ^c −2.01 ^c	0.26 ^c
Cu4'	459 (5.28)			−2.28, −2.05 ^c	0.17, 1.04 ^c
Cu5'	459 (7.35)			−2.35, ^c −1.87 ^c	0.19
Ru1	452 (12.86)	611 (753)	0.09	−2.26, −2.02, −1.80	0.80
Ru2	448 (14.75)	613 (836)	0.15	−2.24, −2.00, −1.78	0.84
Ru3	440 (15.53)	612 (934)	0.27	−2.16, −1.92, −1.73 ^c	0.97 ^c
Ru4	449 (14.58)	613 (1029)	0.40	−2.40, −2.12, −1.84 ^c	0.90
Ru5	445 (13.59)	612 (888)	0.09	−2.40, −2.09, −1.87 ^c	0.87
L1	273 (58.48)	366			
L2	277 (29.1)	366			
L3	274 (43.49)	365			
L4	277 (20.63)	295			
L5	276 (21.1)	365			

^aTaken from ref 23. ^bTaken from ref 55. ^cIrreversible. ^dTaken from ref 28.

functionalized Cu4' and Cu5', both located at 459 nm, are slightly bathochromically shifted compared to Cu1' ($\lambda_{\text{max}} = 455$ nm). In contrast, complexes Cu2' and Cu3' with ether substituents are ~ 340 cm $^{-1}$ hypsochromically shifted (see Table 3). As a major difference, all Ru(II) complexes with additional donor atoms (Ru2–Ru5) absorb stronger than the reference complex Ru1, and the respective MLCT bands are all slightly blue-shifted compared to Ru1. This means that the introduction of additional donor moieties has contrasting effects on the absorption behavior of the Cu(I) and Ru(II) complexes. The additional substituents at the 2 and 9 positions in the phenanthroline seem to lower the absorbance of the Cu(I) complexes but increase the attenuation coefficient of the MLCT bands of the Ru(II) complexes.

The emission behavior was examined in an acetonitrile solution under inert conditions. Under these conditions, all homoleptic Cu(I) complexes Cu1'–Cu5' are not emissive. In contrast, the heteroleptic Cu(I) complexes Cu1–Cu5 emit weakly in an acetonitrile solution with emission maxima between 518 and 551 nm (see Figure 7 and Table 3) and between 508 and 533 nm in the solid state (Figure S6.7 and Table S5). In solution, the emission of the functionalized Cu(I) complexes Cu2–Cu5 is shifted by ~ 623 cm $^{-1}$ to higher energies compared to Cu1 (see Figure 7). In the solid state, a similar trend is observed, except for Cu5 (Figure S6.7). Complex Cu2 (O'Pr) has the strongest emission with an emission quantum yield of 0.23%. Furthermore, the emission lifetime of these complexes is short with $\tau \sim 15$ ns in solution (see Table 3). The emission behavior of the Ru(II) complexes Ru1–Ru5 is clearly different compared to the Cu(I) complexes. Ru1–Ru5 emit in an acetonitrile solution with emission maxima at around 612 nm. Interestingly, no impact of the different substituents is obvious (see Figure 7), and the results are comparable to those of [(bpy)₂Ru(L1)]²⁺ (with bpy = 2,2'-bipyridine).⁵⁴ The emission quantum yields of Ru2–Ru5 are quite low (0.09–0.40%) and on the same order of magnitude as the copper complex Cu2. Instead, the emission

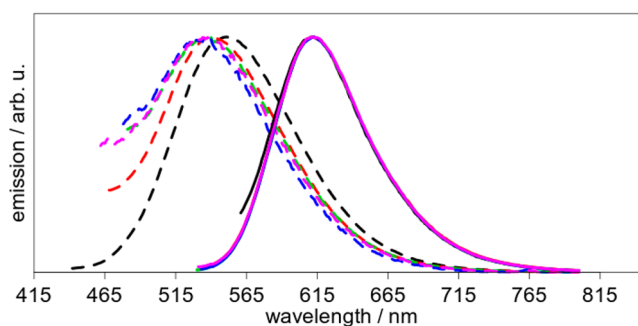


Figure 7. Normalized emission spectra of Cu1 (black, dashed), Cu2 (red, dashed), Cu3 (green, dashed), Cu4 (blue, dashed), and Cu5 (magenta, dashed) and Ru1 (black, solid), Ru2 (red, solid), Ru3 (green, solid), Ru4 (blue, solid), and Ru5 (magenta, solid) in acetonitrile under inert conditions. All complexes are excited at their respective MLCT wavelength.

lifetime is, with ~ 1 μ s, much longer compared to those of Cu1–Cu5 but similar to those of structurally related Ru(II) complexes containing different phenanthroline derivatives (Table 3).⁵⁴

Electrochemical Studies. The electrochemical properties of all complexes were studied by cyclic voltammetry, while Cu2 and Cu2' (both O'Pr) were chosen as representatives of their substance class (for all other cyclic voltammograms, see the SI, Chapter 8). The cyclic voltammograms of the Cu(I) complexes Cu2 and Cu2' possess a reversible reduction event at about -2.05 V versus ferrocene/ferricenium (Fc/Fc⁺) in acetonitrile (see Figure 8, bottom). This reduction is merely shifted by 50 mV to higher potentials compared to the reference Cu1, indicating only a weak influence of the O'Pr substituents. In the case of the homoleptic complex Cu2', a second reduction at -2.26 V occurs.

The thioether (SR, in Cu4, Cu5, Cu4', and Cu5') and ether phenyl (OPh, in Cu3 and Cu3') functionalities lead to an irreversible reduction event. It seems that these ligands are not

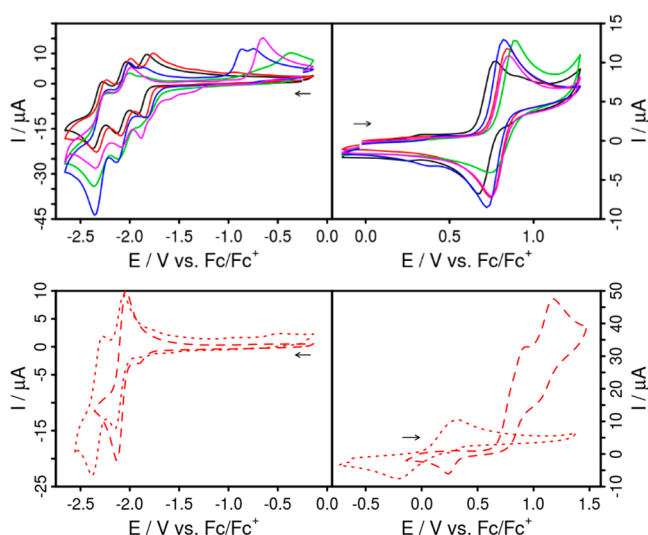


Figure 8. Cyclic voltammograms in an acetonitrile solution with 0.1 M Bu_4NPF_6 as the supporting electrolyte referenced versus a Fc/Fc^+ couple with a scan rate of 100 mV s^{-1} (further scan rates are depicted in the SI, Chapter 8). The arrows illustrate the initial scan direction. Top: Ru(II) complexes **Ru1** (black, solid), **Ru2** (red, solid), **Ru3** (green, solid), **Ru4** (blue, solid), and **Ru5** (magenta, solid). Bottom: Cu(I) complexes **Cu2** (red, dotted) and **Cu2'** (red, dashed).

able to stabilize the negative charge and that a separation of the respective thioether or ether unit occurs (Figures S8.1 and S8.2). For all homoleptic copper complexes **Cu1'**–**Cu5'**, the oxidation at around +0.20 V versus Fc/Fc^+ in acetonitrile (Figures S8.3 and S8.5) is quasi-reversible, except for **Cu3'** (OPh), and can be attributed to oxidation of the copper center from Cu(I) to Cu(II). Moreover, the mild oxidation potentials of $\sim 0.20 \text{ V}$ are rather unusual for such homoleptic bis(diimine)copper(I) complexes.^{2,22} This observation could be explained by a pentacoordinated copper center, which is further supported by the stronger peak separation at higher scan rates (Figures S8.4–S8.7).^{56–58}

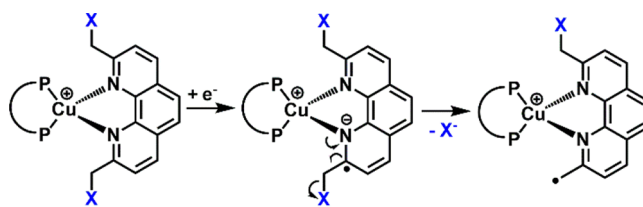
The redox behavior of the ruthenium complexes **Ru1** and **Ru2** is fully reversible (Figure 8). They possess one reversible oxidation and three reversible reductions. The last two reduction events of these Ru(II) complexes can be assigned to the reduction of the two tbbpy ligands⁵³ and the first reduction of the phenanthroline ligand. The introduction of the additional O'Pr donor moiety in **Ru2** causes only a slight shift of 20–40 mV compared to **Ru1** for the first reduction as well as the oxidation (Table 3). Furthermore, the oxidations of all Ru(II) complexes are reversible, except of **Ru3**. In this case the OPh substituents lead to a more pronounced shift of 170 mV. Further, the first reduction processes of **Ru3**–**Ru5** are considerably irreversible and unaffected by the scan rate (Figure S8.12–S8.14), which is in line with the results obtained for the related Cu(I) complexes.

Photostability and Decomposition Studies. The irreversible electrochemical behavior of the Cu(I) complexes containing OPh, S'Pr, or SPh substituents gave a first indication that these compounds possess only a limited stability. Therefore, the photostabilities of representative samples were examined by irradiation of an acetonitrile solution with a xenon lamp (150 W without filter) and continuous monitoring of the absorption spectra (see the SI, Chapter 9). As a result, stepwise decomposition of the heteroleptic Cu(I) complexes **Cu1** and **Cu2** could be

observed. At the same time, the continuous buildup of a new band at around 450 nm (Figures S9.1 and S9.2) is a strong hint for the formation of homoleptic counterparts, which is characteristic for these types of heteroleptic Cu(I) complexes.^{28,32–34} In contrast, upon use of a 360 nm long pass filter (to prevent UV light) and application of a reduced light intensity, complexes **Cu1** and **Cu2** are stable over 2 h (Figures S9.5 and S9.6). Solely, **Cu3** still decomposes to a small extent (Figure S9.7). Most importantly, the homoleptic complexes **Cu1'**–**Cu3'** are fully stable under these conditions (Figures S9.8–S9.10).

As is evident from electrochemistry, **Cu2** (O'Pr) is the only heteroleptic Cu(I) complex with additional donor moieties that showed a reversible reduction. All other copper complexes of this type possess an irreversible behavior under reductive conditions. Therefore, the possible decomposition mechanism and products were investigated in detail to derive new design principles for the future. According to Scheme 2 we assumed

Scheme 2. Proposed Decomposition Mechanism under Reductive Conditions



that, under reductive conditions (either electro- or photochemical), an electron is transferred to the additional donor functionality ($X = \text{OR}$ or SR), leading to cleavage of X^- . This hypothesis was then confirmed by gas chromatography, where the respective decomposition products were found after protonation of the liberated anions with acetic acid. For instance, in the presence of visible light and triethylamine, acting as a reductive quenching agent, phenol (HOPh) was detected as a decomposition product for complex **Cu3** (with OPh). Moreover, the same result was obtained using bulk electrolysis (-1.98 V vs Fc/Fc^+ ; see the SI, Chapter 10) to create reductive conditions. No decomposition was observed for **Cu2** containing the O'Pr substituents (Table S6). Hence, the OPh, S'Pr, or SPh moieties are not able to stabilize an electron at the phenanthroline ligand. The results of the decomposition experiments suggest that the additional donor function X is cleaved as the respective anion X^- . This explains the significantly increased stability of **Cu2** and **Cu2'** (both O'Pr) compared to the other complexes. The isopropoxide anion is much less stable than the other leaving groups, as is evident from the $\text{p}K_a$ values of the corresponding protonated compounds, and is therefore the worst leaving group.^{59–61}

CONCLUSIONS

A new concept to stabilize traditional Cu(I)-based photosensitizers was tested. For this purpose, a systematic series of four 1,10-phenanthroline ligands with two additional group 16 donor functionalities (with $X = \text{OR}$ or SR) were developed. For the first time, these ligands were then coordinated to either the Cu(I) or Ru(II) centers for comparison. In total, 15 complexes, of which 13 are not yet presented in the literature, were prepared. Furthermore, 8 crystal structures could be obtained. X-ray analysis revealed that all homoleptic Cu(I)

complexes **Cu2'**–**Cu5'** possess one Cu–X distance, which is significantly shortened. Therefore, a pentacoordinated copper center, corresponding to a (4 + 1)-fold coordination mode, seems possible.

The introduction of additional substituents (i.e., OⁱPr, OPh, SⁱPr, or SPh) to the phenanthroline had only a slight impact on the absorption maxima. They lowered the absorbance of the Cu(I) complexes but increased the attenuation coefficients of the related Ru(II) complexes. The homoleptic Cu(I) complexes **Cu1'**–**Cu5'** do not show emission in solution, while the heteroleptic Cu(I) complexes **Cu1**–**Cu5** exhibit a weak emission with excited-state lifetimes of about 15 ns. Further, the Ru(II) complexes **Ru2**–**Ru5** are clearly emissive with emission lifetimes of ~1 μs.

The Cu(I) complexes containing thioether (SⁱPr or SPh) or ether aryl (OPh) substituents are not stable under reductive conditions. Only complexes **Cu2** and **Cu2'** with OⁱPr have a reversible reduction at about –2.05 V versus Fc/Fc⁺. All Ru(II) complexes show one reversible oxidation and two reversible reduction events. The limited electrochemical stability of the Cu(I) compounds is in line with a reduced photostability compared to that of the reference complex with no additional donor atoms. Furthermore, under reductive conditions (either by bulk electrolysis or irradiation in the presence of an electron donor like triethylamine), stepwise decomposition of the phenanthroline ligand (i.e., cleavage of the OR or SR substituents) takes place.

Hence, the selected additional donor sites in this study are only partially suited to improve Cu(I)-based photosensitizers. Instead, the application of tetradentate P^NN^NAP⁶² or macrocyclic phenanthroline ligands⁶³ seems more promising and is the focus of our current research.

■ ASSOCIATED CONTENT

SI Supporting Information

The Supporting Information is available free of charge at <https://pubs.acs.org/doi/10.1021/acs.inorgchem.9b03687>.

Experimental and synthetic details, further crystallographic data, NMR, MS, UV/vis, and emission spectra, emission lifetime analysis, cyclic voltammograms, photostability measurements, and details of the degradation studies (PDF)

Accession Codes

CCDC 1972341–1972344, 1972348–1972350, and 1972353 contain the supplementary crystallographic data for this paper. These data can be obtained free of charge via www.ccdc.cam.ac.uk/data_request/cif, or by emailing data_request@ccdc.cam.ac.uk, or by contacting The Cambridge Crystallographic Data Centre, 12 Union Road, Cambridge CB2 1EZ, UK; fax: +44 1223 336033.

■ AUTHOR INFORMATION

Corresponding Authors

Stefanie Tschierlei – Institute of Inorganic Chemistry I, Ulm University, 89081 Ulm, Germany; orcid.org/0000-0001-9441-7904; Email: stefanie.tschierlei@uni-ulm.de

Michael Karnahl – Institute of Organic Chemistry, University of Stuttgart, 70569 Stuttgart, Germany; orcid.org/0000-0002-6755-0002; Email: michael.karnahl@oc.uni-stuttgart.de

Authors

Martin Rentschler – Institute of Organic Chemistry, University of Stuttgart, 70569 Stuttgart, Germany

Marie-Ann Schmid – Institute of Inorganic Chemistry I, Ulm University, 89081 Ulm, Germany

Wolfgang Frey – Institute of Organic Chemistry, University of Stuttgart, 70569 Stuttgart, Germany

Complete contact information is available at:

<https://pubs.acs.org/10.1021/acs.inorgchem.9b03687>

Author Contributions

[†]These authors contributed equally to this work.

Notes

The authors declare no competing financial interest.

■ ACKNOWLEDGMENTS

This work was supported by the Baden-Württemberg Foundation (BW-Stiftung, Germany) and by the Deutsche Forschungs-Gemeinschaft (DFG) within the Priority Program SPP 2102 “Light-controlled reactivity of metal complexes” (TS 330/4-1 and KA 4671/2-1) and the DFG project TS 330/3-1. Special thanks goes to Jannik Brückmann (Ulm) for providing the Ru(II) precursor and to Fiona Schneider (Stuttgart) for preliminary photostability measurements.

■ REFERENCES

- (1) Juris, A.; Balzani, V.; Barigelletti, F.; Campagna, S.; Belser, P.; von Zelewsky, A. Ru(II) polypyridine complexes: photophysics, photochemistry, electrochemistry, and chemiluminescence. *Coord. Chem. Rev.* **1988**, *84*, 85–277.
- (2) Armaroli, N. Photoactive mono- and polynuclear Cu(I)-phenanthrolines. A viable alternative to Ru(II)-polypyridines? *Chem. Soc. Rev.* **2001**, *30* (2), 113–124.
- (3) Eckenhoff, W. T.; Eisenberg, R. Molecular systems for light driven hydrogen production. *Dalton Trans.* **2012**, *41* (42), 13004–13021.
- (4) Frischmann, P. D.; Mahata, K.; Würthner, F. Powering the future of molecular artificial photosynthesis with light-harvesting metallo-supramolecular dye assemblies. *Chem. Soc. Rev.* **2013**, *42* (4), 1847–1870.
- (5) Yuan, Y.-J.; Yu, Z.-T.; Chen, D.-Q.; Zou, Z.-G. Metal-complex chromophores for solar hydrogen generation. *Chem. Soc. Rev.* **2017**, *46* (3), 603–631.
- (6) Bignozzi, C.; Argazzi, R.; Boaretto, R.; Busatto, E.; Carli, S.; Ronconi, F.; Caramori, S. The role of transition metal complexes in dye sensitized solar devices. *Coord. Chem. Rev.* **2013**, *257* (9), 1472–1492.
- (7) Housecroft, C. E.; Constable, E. C. The emergence of copper(i)-based dye sensitized solar cells. *Chem. Soc. Rev.* **2015**, *44* (23), 8386–8398.
- (8) Costa, R. D.; Ortí, E.; Bolink, H. J.; Monti, F.; Accorsi, G.; Armaroli, N. Luminescent Ionic Transition-Metal Complexes for Light-Emitting Electrochemical Cells. *Angew. Chem., Int. Ed.* **2012**, *51* (33), 8178–8211.
- (9) Bizzarri, C.; Spuling, E.; Knoll, D. M.; Volz, D.; Bräse, S. Sustainable metal complexes for organic light-emitting diodes (OLEDs). *Coord. Chem. Rev.* **2018**, *373*, 49–82.
- (10) Prier, C. K.; Rankic, D. A.; MacMillan, D. W. C. Visible Light Photoredox Catalysis with Transition Metal Complexes: Applications in Organic Synthesis. *Chem. Rev.* **2013**, *113* (7), 5322–5363.
- (11) Paria, S.; Reiser, O. Copper in Photocatalysis. *ChemCatChem* **2014**, *6* (9), 2477–2483.
- (12) Schultz, D. M.; Yoon, T. P. Solar Synthesis: Prospects in Visible Light Photocatalysis. *Science* **2014**, *343* (6174), 1239176.

- (13) Ghosh, I.; Marzo, L.; Das, A.; Shaikh, R.; König, B. Visible Light Mediated Photoredox Catalytic Arylation Reactions. *Acc. Chem. Res.* **2016**, *49* (8), 1566–1577.
- (14) Reiser, O. Shining Light on Copper: Unique Opportunities for Visible-Light-Catalyzed Atom Transfer Radical Addition Reactions and Related Processes. *Acc. Chem. Res.* **2016**, *49* (9), 1990–1996.
- (15) Larsen, C. B.; Wenger, O. S. Photoredox Catalysis with Metal Complexes Made from Earth-Abundant Elements. *Chem. - Eur. J.* **2018**, *24* (9), 2039–2058.
- (16) Balzani, V.; Juris, A.; Venturi, M.; Campagna, S.; Serroni, S. Luminescent and Redox-Active Polynuclear Transition Metal Complexes. *Chem. Rev.* **1996**, *96* (2), 759–834.
- (17) Schulz, M.; Karnahl, M.; Schwalbe, M.; Vos, J. G. The role of the bridging ligand in photocatalytic supramolecular assemblies for the reduction of protons and carbon dioxide. *Coord. Chem. Rev.* **2012**, *256* (15), 1682–1705.
- (18) Halpin, Y.; Pryce, M. T.; Rau, S.; Dini, D.; Vos, J. G. Recent progress in the development of bimetallic photocatalysts for hydrogen generation. *Dalton Trans.* **2013**, *42* (46), 16243–16254.
- (19) Kuang, S.-M.; Cuttill, D. G.; McMillin, D. R.; Fanwick, P. E.; Walton, R. A. Synthesis and Structural Characterization of Cu(I) and Ni(II) Complexes that Contain the Bis[2-(diphenylphosphino)phenyl]ether Ligand. Novel Emission Properties for the Cu(I) Species. *Inorg. Chem.* **2002**, *41* (12), 3313–3322.
- (20) Saito, K.; Arai, T.; Takahashi, N.; Tsukuda, T.; Tsubomura, T. A series of luminescent Cu(I) mixed-ligand complexes containing 2,9-dimethyl-1,10-phenanthroline and simple diphosphine ligands. *Dalton Trans.* **2006**, *37*, 4444–4448.
- (21) Luo, S.-P.; Mejía, E.; Friedrich, A.; Pazidis, A.; Junge, H.; Surkus, A.-E.; Jackstell, R.; Denurra, S.; Gladiali, S.; Lochbrunner, S.; Beller, M. Photocatalytic Water Reduction with Copper-Based Photosensitizers: A Noble-Metal-Free System. *Angew. Chem., Int. Ed.* **2012**, *52* (1), 419–423.
- (22) Lazorski, M. S.; Castellano, F. N. Advances in the light conversion properties of Cu(I)-based photosensitizers. *Polyhedron* **2014**, *82*, 57–70.
- (23) Zhang, Y.; Schulz, M.; Wächtler, M.; Karnahl, M.; Dietzek, B. Heteroleptic diimine–diphosphine Cu(I) complexes as an alternative towards noble-metal based photosensitizers: Design strategies, photophysical properties and perspective applications. *Coord. Chem. Rev.* **2018**, *356*, 127–146.
- (24) Leoni, E.; Mohanraj, J.; Holler, M.; Mohankumar, M.; Nierengarten, I.; Monti, F.; Sournia-Saquet, A.; Delavaux-Nicot, B.; Nierengarten, J.-F.; Armaroli, N. Heteroleptic Copper(I) Complexes Prepared from Phenanthroline and Bis-Phosphine Ligands: Rationalization of the Photophysical and Electrochemical Properties. *Inorg. Chem.* **2018**, *57* (24), 15537–15549.
- (25) Sandroni, M.; Pellegrin, Y.; Odobel, F. Heteroleptic bis-diimine copper(I) complexes for applications in solar energy conversion. *C. R. Chim.* **2016**, *19* (1), 79–93.
- (26) Ichinaga, A. K.; Kirchoff, J. R.; McMillin, D. R.; Dietrich-Buchecker, C. O.; Marnot, P. A.; Sauvage, J. P. Charge-transfer absorption and emission of Cu(NN)²⁺ systems. *Inorg. Chem.* **1987**, *26* (25), 4290–4292.
- (27) Sandroni, M.; Kayanuma, M.; Rebarz, M.; Akdas-Kilig, H.; Pellegrin, Y.; Blart, E.; Le Bozec, H.; Daniel, C.; Odobel, F. Heteroleptic diimine copper(I) complexes with large extinction coefficients: synthesis, quantum chemistry calculations and physico-chemical properties. *Dalton Trans.* **2013**, *42* (40), 14628–14638.
- (28) Zhang, Y.; Heberle, M.; Wächtler, M.; Karnahl, M.; Dietzek, B. Determination of side products in the photocatalytic generation of hydrogen with copper photosensitizers by resonance Raman spectroelectrochemistry. *RSC Adv.* **2016**, *6* (107), 105801–105805.
- (29) Mara, M. W.; Fransted, K. A.; Chen, L. X. Interplays of excited state structures and dynamics in copper(I) diimine complexes: Implications and perspectives. *Coord. Chem. Rev.* **2015**, *282–283*, 2–18.
- (30) Mejía, E.; Luo, S.-P.; Karnahl, M.; Friedrich, A.; Tschierlei, S.; Surkus, A.-E.; Junge, H.; Gladiali, S.; Lochbrunner, S.; Beller, M. A Noble-Metal-Free System for Photocatalytic Hydrogen Production from Water. *Chem. - Eur. J.* **2013**, *19* (47), 15972–15978.
- (31) Chen, N.-Y.; Xia, L.-M.; Lennox, A. J. J.; Sun, Y.-Y.; Chen, H.; Jin, H.-M.; Junge, H.; Wu, Q.-A.; Jia, J.-H.; Beller, M.; Luo, S.-P. Structure-Activated Copper Photosensitizers for Photocatalytic Water Reduction. *Chem. - Eur. J.* **2017**, *23* (15), 3631–3636.
- (32) Kaeser, A.; Mohankumar, M.; Mohanraj, J.; Monti, F.; Holler, M.; Cid, J.-J.; Moudam, O.; Nierengarten, I.; Karmazin-Brelot, L.; Duhayon, C.; Delavaux-Nicot, B.; Armaroli, N.; Nierengarten, J.-F. Heteroleptic Copper(I) Complexes Prepared from Phenanthroline and Bis-Phosphine Ligands. *Inorg. Chem.* **2013**, *52* (20), 12140–12151.
- (33) Fischer, S.; Hollmann, D.; Tschierlei, S.; Karnahl, M.; Rockstroh, N.; Barsch, E.; Schwarzbach, P.; Luo, S.-P.; Junge, H.; Beller, M.; Lochbrunner, S.; Ludwig, R.; Brückner, A. Death and Rebirth: Photocatalytic Hydrogen Production by a Self-Organizing Copper-Iron System. *ACS Catal.* **2014**, *4* (6), 1845–1849.
- (34) Nishikawa, M.; Kakizoe, D.; Saito, Y.; Ohishi, T.; Tsubomura, T. Redox Properties of Copper(I) Complex Bearing 4,7-Diphenyl-2,9-dimethyl-1,10-phenanthroline and 1,4-Bis(diphenylphosphino)butane Ligands and Effects of Light in the Presence of Chloroform. *Bull. Chem. Soc. Jpn.* **2017**, *90* (3), 286–288.
- (35) Wallesch, M.; Volz, D.; Zink, D. M.; Schepers, U.; Nieger, M.; Baumann, T.; Bräse, S. Bright Opportunities: Multinuclear CuI Complexes with N-P Ligands and Their Applications. *Chem. - Eur. J.* **2014**, *20* (22), 6578–6590.
- (36) Tschierlei, S.; Karnahl, M.; Rockstroh, N.; Junge, H.; Beller, M.; Lochbrunner, S. Substitution-Controlled Excited State Processes in Heteroleptic Copper(I) Photosensitizers Used in Hydrogen Evolving Systems. *ChemPhysChem* **2014**, *15* (17), 3709–3713.
- (37) Iwamura, M.; Takeuchi, S.; Tahara, T. Ultrafast Excited-State Dynamics of Copper(I) Complexes. *Acc. Chem. Res.* **2015**, *48* (3), 782–791.
- (38) Capano, G.; Chergui, M.; Rothlisberger, U.; Tavernelli, I.; Penfold, T. J. A Quantum Dynamics Study of the Ultrafast Relaxation in a Prototypical Cu(I)-Phenanthroline. *J. Phys. Chem. A* **2014**, *118* (42), 9861–9869.
- (39) Murray, N. S.; Keller, S.; Constable, E. C.; Housecroft, C. E.; Neuburger, M.; Prescimone, A. [Cu(N[^]N)(P[^]P)]⁺ complexes with 2,2':6',2''-terpyridine ligands as the N[^]N domain. *Dalton Trans.* **2015**, *44* (16), 7626–7633.
- (40) Zerk, T. J.; Bernhardt, P. V. Redox-coupled structural changes in copper chemistry: Implications for atom transfer catalysis. *Coord. Chem. Rev.* **2018**, *375*, 173–190.
- (41) Vahrenkamp, H. Sulfur Atoms as Ligands in Metal Complexes. *Angew. Chem., Int. Ed. Engl.* **1975**, *14* (5), 322–329.
- (42) Motoshima, K.; Sato, A.; Yorimitsu, H.; Oshima, K. Efficient Aerobic Oxidation of Phosphines, Phosphites, and Sulfides by Using Trialkylborane. *Bull. Chem. Soc. Jpn.* **2007**, *80* (11), 2229–2231.
- (43) Hernández, D. J.; Vázquez-Lima, H.; Guadarrama, P.; Martínez-Otero, D.; Castillo, I. Solution and solid-state conformations of 1,5-pyridine and 1,5-phenanthroline-bridged p-tert-butylcalix[8]-arene derivatives. *Tetrahedron Lett.* **2013**, *54* (36), 4930–4933.
- (44) Tong, K.-L.; Yee, C.-C.; Tse, Y. C.; Au-Yeung, H. Y. Discoveries from a phenanthroline-based dynamic combinatorial library: catenane from a copper(I) or copper(II) template? *Inorg. Chem. Front.* **2016**, *3*, 348–353.
- (45) Heberle, M.; Tschierlei, S.; Rockstroh, N.; Ringenberg, M.; Frey, W.; Junge, H.; Beller, M.; Lochbrunner, S.; Karnahl, M. Heteroleptic Copper Photosensitizers: Why an Extended π -System Does Not Automatically Lead to Enhanced Hydrogen Production. *Chem. - Eur. J.* **2016**, *23* (2), 312–319.
- (46) McCusker, C. E.; Castellano, F. N. Design of a Long-Lifetime, Earth-Abundant, Aqueous Compatible Cu(I) Photosensitizer Using Cooperative Steric Effects. *Inorg. Chem.* **2013**, *52* (14), 8114–8120.
- (47) Ye, R.-R.; Ke, Z.-F.; Tan, C.-P.; He, L.; Ji, L.-N.; Mao, Z.-W. Histone-Deacetylase-Targeted Fluorescent Ruthenium(II) Polypyridyl Complexes as Potent Anticancer Agents. *Chem. - Eur. J.* **2013**, *19* (31), 10160–10169.

(48) Kroll, A.; Monczak, K.; Sorsche, D.; Rau, S. A Luminescent Ruthenium Azide Complex as a Substrate for Copper-Catalyzed Click Reactions. *Eur. J. Inorg. Chem.* **2014**, *2014* (22), 3462–3466.

(49) Kovalevsky, A. Y.; Gembicky, M.; Novozhilova, I. V.; Coppens, P. Solid-State Structure Dependence of the Molecular Distortion and Spectroscopic Properties of the Cu(I) Bis(2,9-dimethyl-1,10-phenanthroline) Ion. *Inorg. Chem.* **2003**, *42* (26), 8794–8802.

(50) Hartshorn, R. M.; Barton, J. K. Novel dipyrrophenazine complexes of ruthenium(II): exploring luminescent reporters of DNA. *J. Am. Chem. Soc.* **1992**, *114* (15), 5919–5925.

(51) Bolger, J.; Gourdon, A.; Ishow, E.; Launay, J.-P. Mononuclear and Binuclear Tetrapyrrodo[3,2-a:2',3'-c:3'',2''-h:2''',3''-j]phenazine (tpphz) Ruthenium and Osmium Complexes. *Inorg. Chem.* **1996**, *35* (10), 2937–2944.

(52) Karnahl, M.; Kriek, S.; Görls, H.; Tschierlei, S.; Schmitt, M.; Popp, J.; Chartrand, D.; Hanan, G. S.; Groarke, R.; Vos, J. G.; Rau, S. Synthesis and Photophysical Properties of 3,8-Disubstituted 1,10-Phenanthrolines and Their Ruthenium(II) Complexes. *Eur. J. Inorg. Chem.* **2009**, *2009* (33), 4962–4971.

(53) Alkan-Zambada, M.; Keller, S.; Martínez-Sarti, L.; Prescimone, A.; Junquera-Hernández, J. M.; Constable, E. C.; Bolink, H. J.; Sessolo, M.; Ortí, E.; Housecroft, C. E. [Cu(P[^]P)(N[^]N)][PF₆] compounds with bis(phosphane) and 6-alkoxy, 6-alkylthio, 6-phenyloxy and 6-phenylthio-substituted 2,2'-bipyridine ligands for light-emitting electrochemical cells. *J. Mater. Chem. C* **2018**, *6*, 8460–8471.

(54) Yoshikawa, N.; Yamabe, S.; Sakaki, S.; Kanehisa, N.; Inoue, T.; Takashima, H. Transition states of the 3MLCT to 3MC conversion in Ru(bpy)₂(phen derivative)²⁺ complexes. *J. Mol. Struct.* **2015**, *1094*, 98–108.

(55) Phifer, C. C.; McMillin, D. R. The basis of aryl substituent effects on charge-transfer absorption intensities. *Inorg. Chem.* **1986**, *25* (9), 1329–1333.

(56) Rorabacher, D. B. Electron Transfer by Copper Centers. *Chem. Rev.* **2004**, *104* (2), 651–698.

(57) Leovac, V. M.; Rodić, M. V.; Jovanović, L. S.; Joksović, M. D.; Stanojković, T.; Vujčić, M.; Sladić, D.; Marković, V.; Vojinović-Ješić, L. S. Transition Metal Complexes with 1-Adamantoyl Hydrazones – Cytotoxic Copper(II) Complexes of Tri- and Tetradentate Pyridine Chelators Containing an Adamantane Ring System. *Eur. J. Inorg. Chem.* **2015**, *2015* (5), 882–895.

(58) Leite, S. M. G.; Lima, L. M. P.; Gama, S.; Mendes, F.; Orio, M.; Bento, L.; Paulo, A.; Delgado, R.; Iranzo, O. Copper(II) Complexes of Phenanthroline and Histidine Containing Ligands: Synthesis, Characterization and Evaluation of their DNA Cleavage and Cytotoxic Activity. *Inorg. Chem.* **2016**, *55* (22), 11801–11814.

(59) Olmstead, W. N.; Margolin, Z.; Bordwell, F. G. Acidities of water and simple alcohols in dimethyl sulfoxide solution. *J. Org. Chem.* **1980**, *45* (16), 3295–3299.

(60) Bordwell, F. G.; McCallum, R. J.; Olmstead, W. N. Acidities and hydrogen bonding of phenols in dimethyl sulfoxide. *J. Org. Chem.* **1984**, *49* (8), 1424–1427.

(61) Bordwell, F. G.; Hughes, D. L. Thiol acidities and thiolate ion reactivities toward butyl chloride in dimethyl sulfoxide solution. The question of curvature in Bronsted plots. *J. Org. Chem.* **1982**, *47* (17), 3224–3232.

(62) Chen, H.; Xu, L.-X.; Yan, L.-J.; Liu, X.-F.; Xu, D.-D.; Yu, X.-C.; Fan, J.-X.; Wu, Q.-A.; Luo, S.-P. Mononuclear Copper(I) complexes based on phenanthroline derivatives P[^]N[^]N[^]P tetradentate ligands: Syntheses, crystal structure, photochemical properties. *Dyes Pigm.* **2020**, *173*, 108000.

(63) Brandl, T.; Kerzig, C.; Le Pleux, L.; Prescimone, A.; Wenger, O.; Mayor, M. Improved Photostability of a Cu(I) Complex by Macrocyclization of the Phenanthroline Ligands. *Chem. - Eur. J.* **2020**, *26*, 3119.